

# Characterization of Corneal Biomechanical Properties and Determination of Natural Intraocular Pressure Using CID-GAT

Shu-Hao Lu<sup>1</sup>, I. T. Chong<sup>1</sup>, Stanley Y. Y. Leung<sup>1</sup>, and David C. C. Lam<sup>1</sup>

<sup>1</sup>Department of Mechanical and Aerospace Engineering, The Hong Kong University of Science and Technology, Hong Kong, China

Correspondence: David C. C. Lam, Department of Mechanical and Aerospace Engineering, The Hong Kong University of Science and Technology, Clear Water Bay, Hong Kong 852, China. e-mail: medclam@ust.hk

Received: 23 May 2019

Accepted: 13 July 2019

Published: 11 September 2019

**Keywords:** intraocular pressure; biomechanical properties; corneal modulus; confounding factors; porcine eyes

**Citation:** Lu S-H, Chong IT, Leung SY, Lam DCC. Characterization of corneal biomechanical properties and determination of natural intraocular pressure using CID-GAT. *Trans Vis Sci Tech.* 2019;8(5):10, <https://doi.org/10.1167/tvst.8.5.10> Copyright 2019 The Authors

**Purpose:** The intraocular pressure (IOP) measured using Goldmann Applanation Tonometry (GAT) is confounded by individual corneal properties. We investigated a modified method that removes the confoundment by incorporating corneal properties into the Imbert-Fick's law is investigated.

**Method:** Porcine eyes were pressurized between 10 and 40 mm Hg using a manometer. The eyes were indented using a flat cylindrical indenter. A modified corneal indentation device (CID) procedure was used to obtain the corneal moduli  $E_{qs}$ . The calculated IOP<sub>NC</sub> from the Imbert-Fick's Law using the corneal moduli  $E_{qs}$  was compared to the natural IOP<sub>N</sub>, measured using pressure sensor inserted into the eye.

**Results:** Test results showed that IOP-dependent corneal modulus  $E_{qs}$  is a primary confounding factor in IOP calculation. The average elastic modulus  $E_{qs}$  is  $0.173 \pm 0.018$  MPa at 20 mm Hg, and increases with IOP at a linear rate of 0.0066 MPa per mm Hg ( $r = 0.997$ ,  $P < 0.001$ ). Incorporation of individual  $E_{qs}$  into IOP<sub>NC</sub> calculation showed that IOP<sub>NC</sub> are in good agreement with reference IOP<sub>N</sub> (slope = 0.999,  $r = 0.939$ ,  $P < 0.001$ ).

**Conclusions:** The IOP-dependent corneal modulus  $E_{qs}$  is a primary confounding factor in IOP calculation. A modified CID-GAT procedure to obtain natural cornea-independent IOP<sub>NC</sub> is developed and verified in this study. The CID-GAT IOP modification may be used in place of conventional GAT when the confounding effects in eyes with atypical cornea (e.g., laser-assisted in situ keratomileusis [LASIK] thinned) are significant.

**Translational Relevance:** Confoundment from corneal properties results in IOP measurement errors. The study showed that the CID-GAT method can significantly reduce the confounding corneal errors.

## Introduction

The accuracy of Goldmann applanation tonometry (GAT) is confounded by individual variations, such as central corneal thickness (CCT), corneal radius of curvature, and elastic modulus.<sup>1–9</sup> Confoundment by these parameters leads to >3 mm Hg error in the measurement.<sup>9–13</sup> The majority of the geometric parameters, including CCT and curvature, can be measured in vivo, and methodologies to account for these geometric parameters in GAT intraocular pressure (IOP) have been developed.<sup>9</sup> Despite these advances, a gap between the GAT and

natural (IOP<sub>N</sub>) IOP in the eye remains because of the inability to account for individual biomechanical properties in the GAT IOP.

GAT measures the corneal applanation load at a fixed area  $A$  and calculates the IOP using the Imbert-Fick's law.<sup>14</sup> During applanation, the applanation force  $F$  is opposed by the surface tension  $s$  from the tear film, upward corneal resistance  $b$ , and outward IOP. The force balance is given as Equation 1.

$$\text{IOP} = \frac{F + s - b}{A}. \quad (1)$$

The method is valid only when the corneal

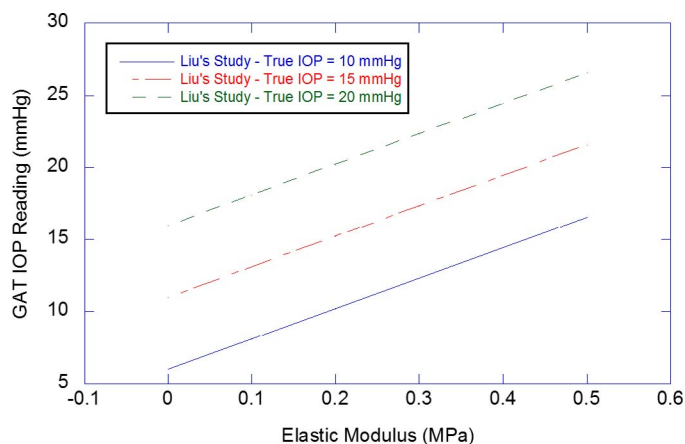


**Figure 1.** Theoretical prediction of the influence of corneal biomechanics on IOP measurement by Liu et al.<sup>8</sup>

resistance  $b$  cancels out the corneal surface tension  $s$ . Mechanics analysis<sup>15,16</sup> showed that the individual corneal resistance  $b$  is not a constant, but is a function of the corneal thickness  $t$ , anterior cornea curvature  $R_c$ , indentation depth  $\delta$ , geometric parameter  $a$ , Poisson's ratio  $\nu$ , and Goldmann quasistatic elastic modulus  $E_{GAT}$ , given as:

$$b = \frac{E_{GAT} t^2}{a(R_c - t/2)\sqrt{1 - \nu^2}} \delta. \quad (2)$$

Goldmann and Schmidt<sup>14</sup> examined the corneal applanation behavior on a group of patients. The study determined that the population-averaged  $b$  is counterbalanced by  $s$  at the GAT applanation contact area  $A_{GAT} = 7.35 \text{ mm}^2$  (applanation diameter of 3.06 mm) such that,

$$\text{IOP}_{GAT} = \frac{F}{A_{GAT}}. \quad (3)$$

The simplification is acceptable when the corneal resistance of the subject is the same as assumed in the formulation, but IOP measurement on subjects with corneal properties different from that assumed in GAT will lead to measurement errors.<sup>4</sup> The error has been theoretically examined by Liu et al.<sup>8</sup> They showed that when the elastic modulus is halved or doubled, up to 5 mm Hg of error may occur (Fig. 1). In further work by others,<sup>16–18</sup> the corneal behavior is shown to be nonlinear viscoelastic, such that the effective elastic modulus is dependent on the IOP and loading rate (Fig. 2). In Goldmann applanation, the load is measured after the applanation is stabilized. Under this quasistatic condition, the  $E_{GAT}$  measured in GAT is a quasistatic property. Estimates in the literature showed that corneal property is a con-

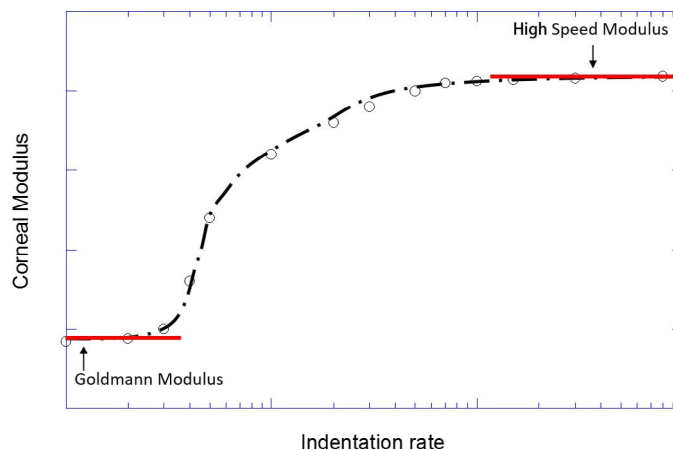


**Figure 2.** Corneal tangent modulus as a function of indentation rate for a porcine eye.<sup>16</sup>

founder factor that could result in IOP error of up to 5.35 mm Hg<sup>4</sup> in GAT.

In this study, a new method to measure the corneal properties of test eyes and an analysis method to determine the corneal-independent  $\text{IOP}_N$  are developed and tested using porcine eyes.

## Methods

In prior studies, indentation methodologies were developed to characterize high-speed indentation behavior of the eyes.<sup>16–18</sup> The instrumented corneal indentation was used to characterize load-displacement data at high speed for eyes pressurized between 20 mm Hg and 40 mm Hg. The procedure was tested on porcine eyes ex vivo and rabbit eyes in vivo. The corneal indentation device (CID, Fig. 3) was developed from these earlier studies and was designed to indent the cornea using a flat punch indenter; the

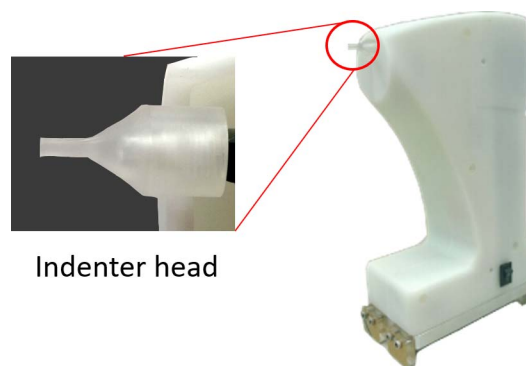


**Figure 3.** Corneal indentation device and corneal indenter (US Patent WO2012163080 A, 2012).

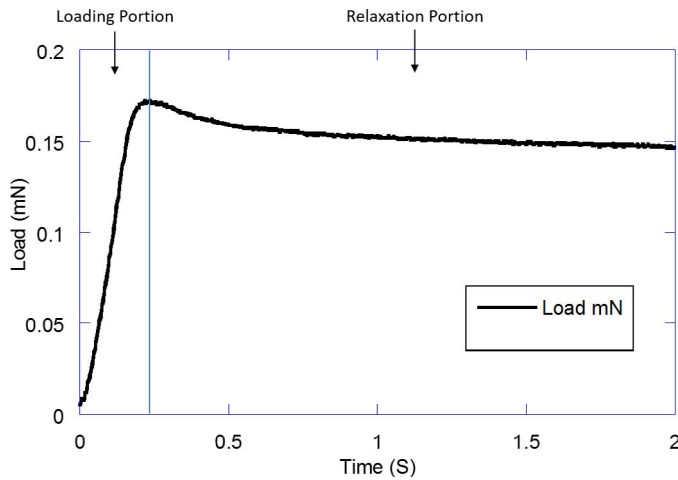


**Figure 4.** Fast indentation loading and relaxation of indented load on porcine eyes.

loads and displacements are recorded during corneal indentation. The CID was deployed successfully in clinical trials to characterize the in vivo corneal tangent modulus<sup>16–18</sup> in humans. In CID tests on porcine eyes, the indentation load becomes stable at fixed displacement after the displacement is held for 2 or more seconds (Fig. 4). The stabilized CID quasistatic load is fully relaxed, and the load measured under this condition corresponds directly with the quasistatic load in GAT. The quasistatic stiffness of the eye then is the change in quasistatic load per unit indent depth. The procedure to characterize the quasistatic stiffness as a function of

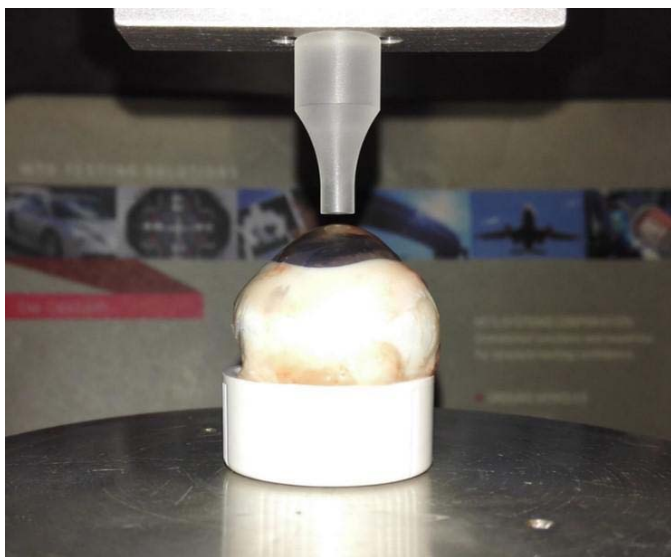


**Figure 5.** Experimental setups on porcine eyes.

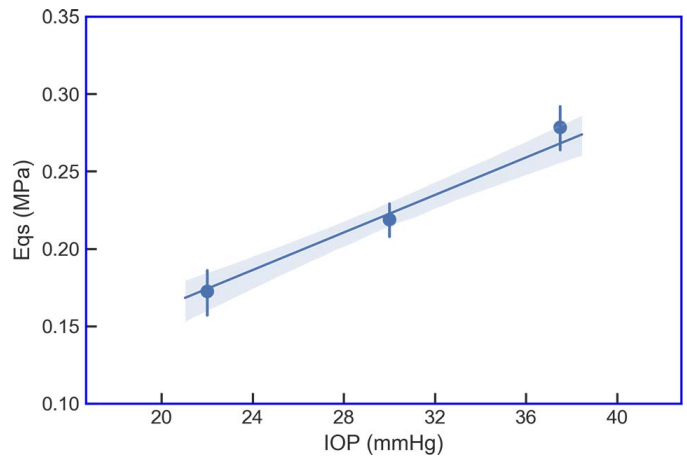


**Figure 6.** Goldmann tangent modulus in the function IOP on porcine eyes.

IOP under the quasistatic Goldmann condition is detailed below.

We tested 15 fresh ex vivo porcine eyes in indentation tests in this study. Porcine eyes were obtained from a local abattoir, and kept moist and cold using an insulated bucket with refrigerants. All experiments were conducted within 12 hours of the animals being killed.

Before testing, the porcine eye with muscle and adipose tissue attached was placed on a support cup fixture. A hypodermic needle, connected to a manometer, was inserted into the anterior chamber of the eye. The pressure  $P_m$  was adjusted between 10 and 40 mm Hg by adjusting the liquid level in the manometer and calculated using,

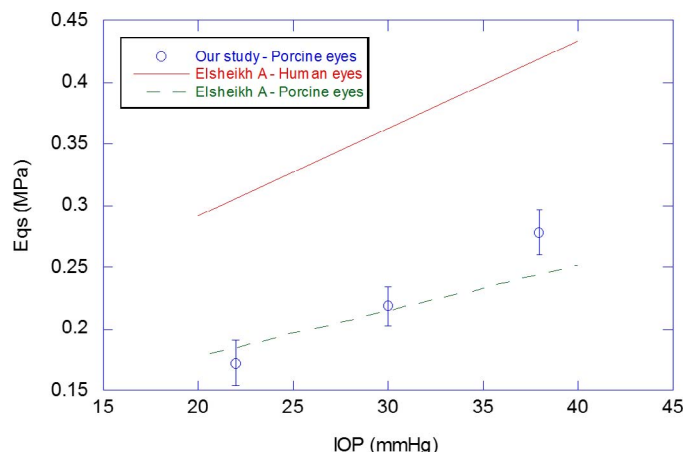


**Figure 7.** Comparison of quasistatic tangent modulus with Elsheikh’s study.<sup>3</sup>

**Table 1.** Determination of the Coefficient: The Empirical Geometry Coefficient  $a$  can be Determined From the Look-Up Table Using the Value of Indentation Geometry Constant  $\mu$  (Equation 7)

$\mu$	0	0.1	0.2	0.4	0.6	0.8	1.0	1.2	1.4
$a$	0.443	0.431	0.425	0.408	0.386	0.362	0.337	0.311	0.286

$$P_m = \rho gh, \tag{4}$$

where  $\rho$  is the density of the fluid (water) in the manometer,  $g$  is the gravitational acceleration, and  $h$  is the height difference between the hypodermic needle and liquid level in the manometer. A needle pressure sensor was inserted into the anterior chamber to monitor the reference IOP<sub>N</sub> in the chamber synchronously as feedback.

The pressurized porcine eyes were indented using the CID with a 3.5 mm flat punch indenter (Fig. 5). The eyes were indented to full contact by the 3.5 mm flat punch at a rate of 12 mm/s to set depths of  $\delta_p = 0.4$  and 0.6 mm, respectively. The displacements were held for four seconds at each set depth until the load became steady (Fig. 4). The load-displacement and time data were captured at a sampling rate of 333 Hz (1 sampling point/0.003 second) by the CID and stored.

In indentation tests, the cornea is deformed by the indentation load and IOP. At full indenter contact, the indentation resistance is described by Equation 2, and the force balance on the indenter can be modeled using the Imbert-Fick's law (Equation 1). Rearranging,

$$E|_{IOP} = \frac{dF/d\delta|_{IOP}}{K_g} = \frac{s|_{IOP}}{K_g}, \tag{5}$$

the indentation modulus at constant IOP as  $E|_{IOP}$  can be derived from the corneal stiffness,  $s|_{IOP}$  is the corneal stiffness.  $K_g$  is,

$$K_g = \frac{t^2}{a(R_c - t/2)\sqrt{1 - \nu^2}} \tag{6}$$

where  $R_c$  is the anterior corneal radius of curvature (outermost surface),  $t$  is the central corneal thickness,  $\nu$  is the Poisson's ratio of the cornea ( $\nu \sim 0.5$ <sup>19</sup>), and  $a$  is the empirical geometry coefficient, determined from indentation geometry constant  $\mu$  and Table 1,<sup>15</sup>

$$\mu = r_0 \left[ \frac{12(1 - \nu^2)}{(R - t/2)^2 t^2} \right]^{1/4}, \tag{7}$$

where  $r_0$  is the radius of the contact area between the indenter and cornea.

After complete relaxation at the two displacements  $\delta_{p,1}$  and  $\delta_{p,2}$ , the individual  $E_{GAT}$  were determined from the two stabilized loads and displacements using,

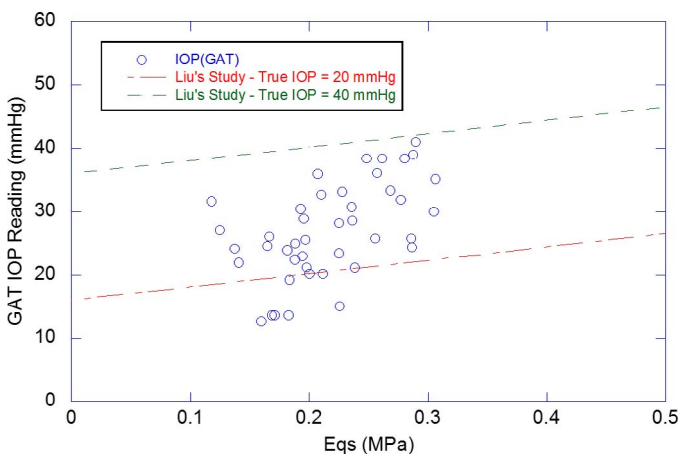


**Figure 8.** Comparison of GAT IOP readings in the function of Goldmann quasistatic modulus with Liu's study.<sup>8</sup>

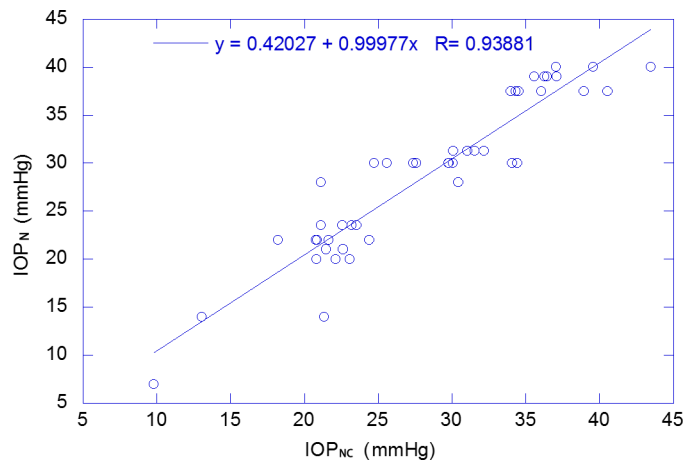


**Figure 9.** Correlation of modified IOP versus controlled IOP on porcine eyes.

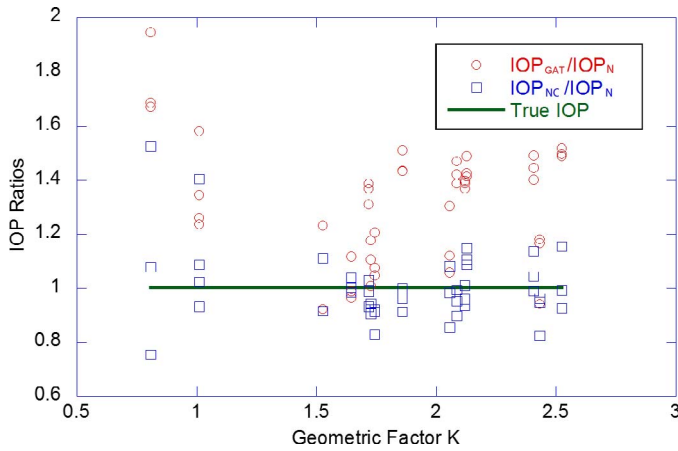


**Figure 10.** Measured IOP/true IOP ratio in the function of geometric factor  $K_g$ .

$$E_{GAT} = \frac{dF/d\delta|_{GAT}}{K_g} = \frac{F_{p,1} - F_{p,2}}{\delta_{p,1} - \delta_{p,2}} / K_g. \quad (8)$$

The corneal bending resistance then is determined by substituting Equation 8 into Equation 2. The specific surface tension  $s$  can be determined by the diameter of the contact area between the indenter and the cornea,

$$s = s_{GAT} \frac{D}{D_{GAT}}, \quad (9)$$

where  $s_{GAT}$  is the tear surface tension at  $A_{GAT} = 7.35 \text{ mm}^2$  ( $s_{GAT} \approx 0.00407115N^{2,8}$ ),  $D$  is the diameter of the indenter, and  $D_{GAT}$  is 3.06 mm.

$IOP_{NC}$  is computed using the Imbert-Fick's law in Equation 1 while the GAT IOP was determined by Equation 3 where the appplanation area was set to  $3.06 \text{ mm}^2$ . The corneal dependence of IOP was

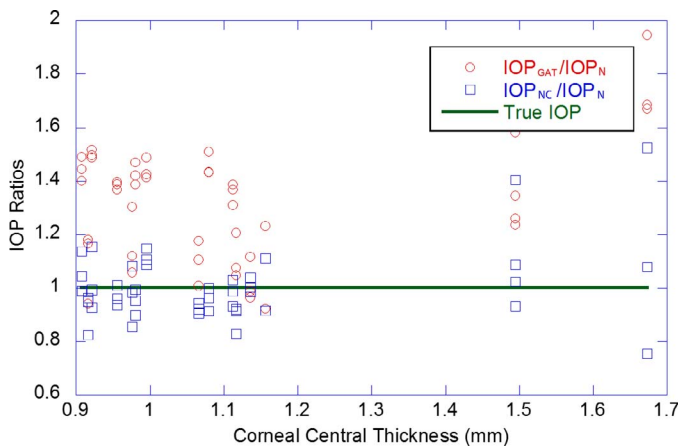


**Figure 11.** Measured IOP/true IOP ratio in the function of corneal central thickness.

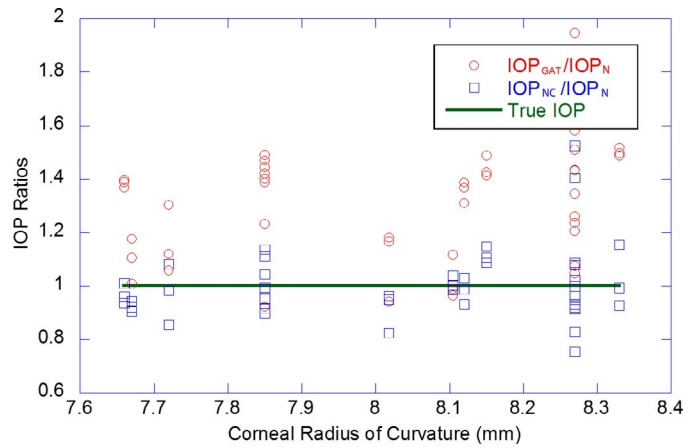


**Figure 12.** Measured IOP/true IOP ratio in the function of corneal radius of curvature.

examined by comparing  $IOP_{NC}$  with the reference  $IOP_N$ .

## Results

The Goldmann elastic modulus from the quasistatic stiffness in Equation 5 is shown in Figure 6. The average elastic modulus  $E_{qs}$  is  $0.173 \pm 0.018 \text{ MPa}$  at IOP of 20 mm Hg. The magnitudes are comparable with Elsheikh's study using the inflation test where corneas also were loaded in a quasistatic manner (Fig. 7).<sup>3,8</sup> The Figures show the  $E_{qs}$  varied linearly with IOP such that an increment of each mm Hg in IOP results in an  $E_{qs}$  change of 0.0066 MPa ( $r = 0.997$ ,  $P < 0.001$ ). The quasistatic corneal modulus  $E_{qs}$  doubles if the IOP is increased by 25 mm Hg. The results are in agreement with the theoretical estimates reported in the study by

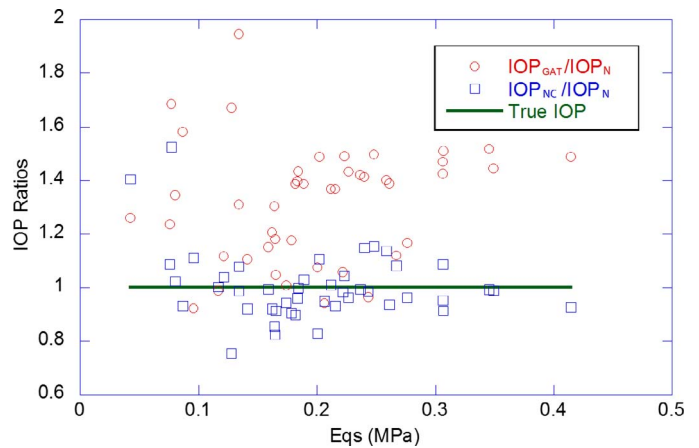


**Figure 13.** Measured IOP/true IOP ratio in the function of Goldmann elastic modulus  $E_{qs}$ .

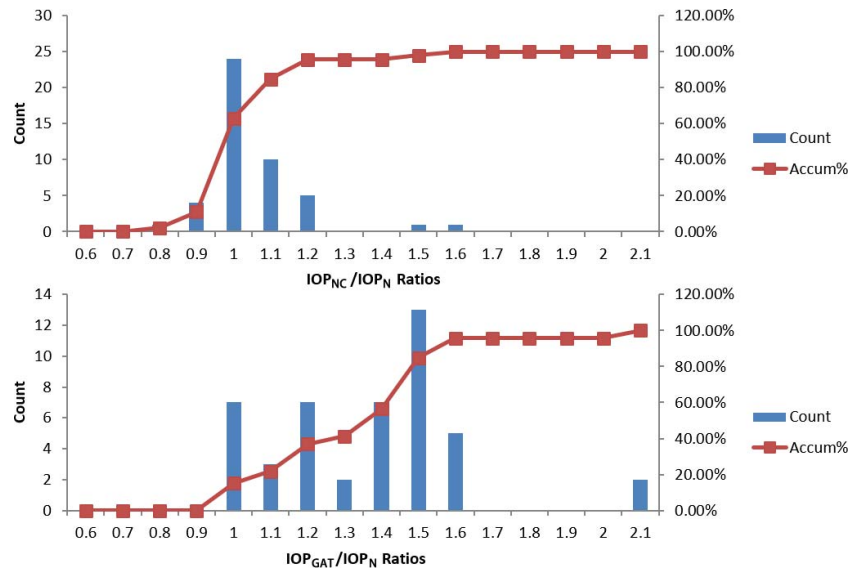


**Figure 14.** Comparison of corneal-independent IOP and GAT IOP measurement.

Liu et al.<sup>8</sup> (Fig. 8). Comparison of  $IOP_{NC}$ , calculated using individual  $E_{qs}$ , with reference  $IOP_N$  is plotted in Figure 9. Analysis showed that  $IOP_{NC}$  is in good agreement with  $IOP_N$  ( $n = 15$ ,  $r = 0.94$ ,  $P < 0.001$ ). This shows that the CID-GAT procedure and the modified calculation method successfully removed the confounding effect from the cornea from  $IOP_{NC}$ .

## Discussion

The good agreement between  $IOP_{NC}$  and reference  $IOP_N$  is dependent on the ability of the CID to characterize the quasistatic  $E_{qs}$  of the cornea. Asejczyk-Widlicka et al.<sup>20</sup> reported a corneal elastic modulus of 0.05 to 0.24 MPa in the IOP range from 12 to 25 mm Hg on porcine eyes ex vivo.<sup>20</sup> Inflation tests were conducted in their study, but the rates were not specified. Elsheikh et al.<sup>3</sup> performed inflation tests on human and porcine eyes. In their tests, the eyes were quasistatically loaded to set pressure and with similar loading conditions to our study. The corneal quasistatic tangent moduli determined in their inflation tests of porcine eyes (dashed line) are in the same range of results as the present study shown in Figure 7.

The confounding effects of corneal properties in GAT IOP measurement were examined quantitatively by Liu et al.<sup>8</sup> They investigated the IOP elevation in porcine eyes after glutaraldehyde treatment and found that the corneal modulus increased 1 MPa for every 5 mm Hg change in IOP.<sup>21</sup> Our results are in

line with their model over the tested range of pressure (Fig. 8).

The confounding effect of the geometric factor  $K_g$ , corneal center thickness, corneal radius, and  $E_{qs}$  on IOP are shown in Figures 10 to 13, respectively. The variation between the  $IOP_N$  and  $IOP_{GAT}$  indicates the dependencies of GAT measurement on these corneal properties. Comparison (Fig. 14) showed that the standard deviation ( $SD = 0.11$ ) of  $IOP_{NC}$  from  $IOP_N$  was significantly smaller than that ( $SD = 0.32$ ) of the  $IOP_{GAT}$  from  $IOP_N$ . More than 80% of  $IOP_{NC}$  were within 10% error of  $IOP_N$  while  $IOP_{GAT}$  generally deviated from  $IOP_N$  by 50%.

The CID-GAT method was designed to characterize the  $IOP_N$  by accounting for the effects of individual-specific corneal biomechanical properties and corneal geometries on  $IOP_N$ . Changes in corneal curvature ( $R_c$ ), thickness ( $t$ ), and corneal elastic properties ( $E_{qs}$ ) were accounted for in Equation 6. The corneal elastic properties (i.e., the elastic modulus of the tissue) are known to increase with aging and IOP.<sup>22–25</sup> The curvature and corneal modulus may change in subjects with keratoconus, and the corneal thickness may increase in subjects with edematous corneas. These confounding effects from aging or illnesses are readily accounted for by the CID-GAT method in Equation 6.

In conclusion, the confounding effect of corneal properties has a great impact on GAT IOP measurement. The effect can be reduced significantly using the CID-GAT method with an updated treatment for corneal resistance in the Imbert-Fick's Law. The

updated calculation of IOP<sub>NC</sub> using corneal modulus obtained from the CID showed good agreement with IOP<sub>N</sub>, the natural IOP of the eye. The CID-GAT method to calculate IOP<sub>N</sub> may be of particular relevance and use for subjects with corneas having abnormal biomechanical properties (e.g., aging effects, refractive surgeries, swelling, keratoconus, and so forth).

## Acknowledgments

Disclosure: **S.-H. Lu**, None; **I.T. Chong**, None; **S.Y.Y. Leung**, None; **D.C.C. Lam**, None

## References

1. Chihara E. Assessment of true intraocular pressure: the gap between theory and practical data. *Surv Ophthalmol*. 2008;53:203–218.
2. Damji KF, Muni RH, Munger RM. Influence of corneal variables on accuracy of intraocular pressure measurement. *J Glaucoma*. 2003;12:69–80.
3. Elsheikh A, Alhasso D, Rama P. Biomechanical properties of human and porcine corneas. *Exp Eye Res*. 2008;86:783–790.
4. Hamilton KE, Pye DC. Young's modulus in normal corneas and the effect on applanation tonometry. *Optom Vis Sci*. 2008;85:445–450.
5. Krueger RR, Ramos-Esteban JC. How might corneal elasticity help us understand diabetes and intraocular pressure? *J Refract Surg*. 2007;23:85–88.
6. Kwon T, Ghaboussi J, Pecknold D, Hashash Y. Effect of cornea material stiffness on measured intraocular pressure. *J Biomech*. 2008;41:1707–1713.
7. Lim T-C, Chattopadhyay S, Acharya UR. A survey and comparative study on the instruments for glaucoma detection. *Med Eng Phys*. 2012;34:129–139.
8. Liu J, Roberts CJ. Influence of corneal biomechanical properties on intraocular pressure measurement: quantitative analysis. *J Cataract Refract Surg*. 2005;31:146–155.
9. Orsengo GJ, Pye DC. Determination of the true intraocular pressure and modulus of elasticity of the human cornea in vivo. *Bull Math Biol*. 1999;61:551–572.
10. Ehlers N, Bramsen T, Sperling S. Applanation tonometry and central corneal thickness. *Acta Ophthalmol*. 1975;53:34–43.
11. Whitacre MM, Stein RA, Hassanein K. The effect of corneal thickness on applanation tonometry. *Am J Ophthalmol*. 1993;115:592–596.
12. Doughty MJ, Zaman ML. Human corneal thickness and its impact on intraocular pressure measures: a review and meta-analysis approach. *Surv Ophthalmol*. 2000;44:367–408.
13. Kohlhaas M, Boehm AG, Spoerl E, Pürsten A, Grein HJ, Pillunat LE. Effect of central corneal thickness, corneal curvature, and axial length on applanation tonometry. *Arch Ophthalmol*. 2006;124:471–476.
14. Goldmann H, Schmidt T. Über applanationstonometrie. *Ophthalmologica*. 1957;134:221–242.
15. Young WC, Budynas RG. *Roark's Formulas for Stress & Strain*. 7th ed. New York: McGraw-Hill; 2002:1–852.
16. Ko MW, Leung LK, Lam DC, Leung CK. Characterization of corneal tangent modulus in vivo. *Acta Ophthalmol*. 2013;91:e263–e269.
17. Ko MW, Leung LK, Lam DC. Partial contact indentation tonometry for measurement of corneal properties-independent intraocular pressure. *Mol Cell Biomech*. 2012;9:251–268.
18. Leung LK, Ko MW, Lam DC. Individual-specific tonometry on porcine eyes. *Med Eng Phys*. 2014;36:96–101.
19. Kampmeier J, Radt B, Birngruber R, Brinkmann R. Thermal and biomechanical parameters of porcine cornea. *Cornea*. 2000;19:355–363.
20. Asejczyk-Widlicka M, Pierscionek B. The elasticity and rigidity of the outer coats of the eye. *Br J Ophthalmol*. 2008;92:1415–1418.
21. Liu J, He X. Corneal stiffness affects IOP elevation during rapid volume change in the eye. *Invest Ophthalmol Vis Sci*. 2009;50:2224–2229.
22. Leung LK, Ko MW, Lam DC. Effect of age-stiffening tissues and intraocular pressure on optic nerve damages. *Mol Cell Biomech*. 2012;9:157–173.
23. Pepose JS, Feigenbaum SK, Qazi MA, Sanderson JP, Roberts CJ. Changes in corneal biomechanics and intraocular pressure following LASIK using static, dynamic, and noncontact tonometry. *Am J Ophthalmol*. 2007;143:39–47.
24. Ortiz D, Piñero D, Shabayek MH, Arnalich-Montiel F, Alió JL. Corneal biomechanical properties in normal, post-laser in situ keratomileusis, and keratoconic eyes. *J Cataract Refract Surg*. 2007;33:1371–1375.
25. Hatami-Marbini H, Etebu E. Hydration dependent biomechanical properties of the corneal stroma. *Exp Eye Res*. 2013;116:47–54.